



Contents lists available at ScienceDirect

Surface Science

journal homepage: www.elsevier.com/locate/susc

Q3 Reconstruction of low-index graphite surfaces

Q4 Sascha Thinius, Mazharul M. Islam, Thomas Bredow*

Mulliken Center for Theoretical Chemistry, Institut für Physikalische und Theoretische Chemie, Universität Bonn, Beringstr. 4, 53115 Bonn, Germany

ARTICLE INFO

Article history:

Received 17 December 2015

Accepted 31 January 2016

Available online xxx

Keywords:

Density functional theory

Dispersion correction

Surface reconstruction

Graphite

Surface energy

Wulff construction

ABSTRACT

The low-index graphite surfaces $(10\bar{1}0)$, $(10\bar{1}1)$, $(11\bar{2}0)$ and $(11\bar{2}1)$ have been studied by density functional theory (DFT) including van-der-Waals (vdW) corrections. Different from the (0001) surface which has been extensively investigated both experimentally and theoretically, there is no comprehensive study on the $(10\bar{1}0)$ - $(10\bar{1}1)$ -, $(11\bar{2}0)$ - and $(11\bar{2}1)$ -surfaces available, although they are of relevance for Li insertion processes, e.g. in Li-ion batteries. In this study the structure and stability of all non- (0001) low-index surfaces were calculated with RPBE-D3 and converged slab models. In all cases reconstruction involving bond formation between unsaturated carbon atoms of two neighboring graphene sheets reduces the surface energy dramatically. Two possible reconstruction patterns have been considered. The first possibility leads to formation of oblong nanotubes. Alternatively, the graphene sheets form bonds to different neighboring sheets at the upper and lower sides and sinusoidal structures are formed. Both structure types have similar stabilities. Based on the calculated surface energies the Gibbs–Wulff theorem was applied to construct the macroscopic shape of graphite single crystals.

© 2016 Elsevier B.V. All rights reserved.

1. Introduction

Graphite is a widely used material in technology and research. Its application area ranges from carbon filters, admixtures for steel, high-temperature, composite, non-corrosive materials and fibers to electrodes, lithium-battery anode materials (e.g. LiC_6), super-conducting intercalation compounds (e.g. KC_8 , CaC_6) as well as graphene, fullerenes, nanotubes, -ribbons and -rods.

The structure of graphite belongs to space group $P6_3/mmc$ with cell parameters $a = 2.464$ and $c = 6.771$ Å. The unit cell is depicted in Fig. 1. It contains two carbon atoms at sites $C1 = (0, 0, 3/4)$ and $C2 = (1/3, 2/3, 1/4)$ [1]. The layers in crystallographic c -direction are stacked in an AB sequence, where the atoms of the B -layer are shifted by $1/3$ of the lattice vectors \mathbf{a} and \mathbf{b} w.r.t. the atoms of the A -layers.

It is well known that the stability of graphite originates from its hexagonal honeycomb lattice, the graphene sheets, which are parallel to the (0001) lattice plane and interconnected mainly by London dispersion forces. There are many experimental and theoretical studies on this surface (see reviews [2,3,4,5,6], text books [7,8] and references therein). But since graphite is a three-dimensional material, also other surfaces must exist determining the macroscopic crystal shape. Due to hexagonal symmetry the number of low-index surfaces is reduced to five planes, namely (0001) , $(10\bar{1}0) = (01\bar{1}0)$, $(10\bar{1}1) = (01\bar{1}1)$, $(11\bar{2}0)$ and $(11\bar{2}1)$.

Since it is well known that Li diffusion through the (0001) planes is hindered by large barriers [9], Li intercalation of graphite particles must proceed either via defects in the (0001) plane or via the open non- (0001) surfaces. For this reason knowledge of the corresponding surface structures and stabilities is of relevance e.g. in battery research. To our knowledge, there is no theoretical or experimental study classifying the non- (0001) -surfaces energetically. With this work we intend to close this gap by applying density-functional theory (DFT) and converged slab models. First the surface energies are calculated for the relaxed but non-reconstructed surfaces. In a second step the surfaces are forced to reconstruct in two ways, leading to two configurations denoted as oval (o) and sinusoidal (s).

This approach was inspired by the reverse unzipping process [10] of carbon nanotubes and capped carbon nanotubes [11,12,13]. Experimentally this kind of reconstruction has been observed by scanning tunneling spectroscopy (STM) [14,15,16,17] at highly ordered pyrolytic graphite (HOPG) surfaces due to interaction with the STM tip, by transmission electron microscopy (TEM) of graphite nanoparticles [18], graphite polyhedral crystals (GPCs) [19,20], nanotubes [21,22], HOPG [23], graphene bilayers [24,25] and graphite filaments [26,27,28,29,30,31]. Theoretically, the formation of capped surface edges has been studied for graphite nanoparticles [18] with molecular dynamics (MD) techniques, showing that there are a variety of possible reconstruction patterns but without providing details about geometry and energetics of the surfaces. Previous studies [20,18,21,27,28,29,31] show that also double and multilayer arches can be formed. This could further minimize the ring tension of the reconstructed structures. Also interlinking between reconstructed double and multiple layers has been observed by MD simulations [18].

* Corresponding author. Tel.: +49 228 73 3839; fax: +49 228 73 9064.
E-mail address: bredow@thch.uni-bonn.de (T. Bredow).

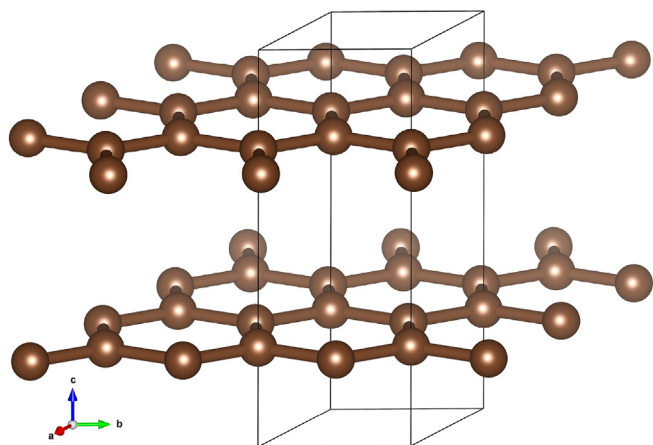


Fig. 1. Part of the graphite bulk showing the layered honeycomb structure. Black lines: conventional unit cell.

2. Computational methods

The structural and energetic properties of the graphite surfaces were calculated with periodic DFT and DFT-D3-BJ methods. The revised Perdew–Burke–Ernzerhof (RPBE) functional [32,33,34] was employed. For all calculations the plane-wave program VASP [35,36,37,38,39] and the projector-augmented wave (PAW) method [40,39] were used. The same computational setup was used in a previous study of Li intercalation in graphite [9] and was chosen due to its high accuracy for structural properties. We used a converged energy cutoff value of $E_{\text{cut}} = 900$ eV for bulk and surface calculations.

The surface calculations were performed with a 10 Å vacuum separation of the slabs which was tested to guarantee negligible surface–surface interaction. Integration in reciprocal space was performed with gamma-centered Monkhorst–Pack grids $24 \times 24 \times 12$, $21 \times 21 \times 1$, $22 \times 11 \times 1$, $19 \times 19 \times 1$, $26 \times 13 \times 1$ and $15 \times 15 \times 1$ for bulk graphite and (0001)-, (10 $\bar{1}$ 0)-, (10 $\bar{1}$ 1)-, (11 $\bar{2}$ 0)- and (11 $\bar{2}$ 1)-slabs, respectively. An energy convergence of 10^{-5} eV/atom was achieved with these settings.

The effect of London dispersion forces between the carbon layers was taken into account by the DFT-D3-BJ method of Grimme et al. [41] which features the Becke–Johnson damping scheme [42,43].

With these settings the graphite lattice parameters are obtained as $a = 2.469$ Å and $c = 6.691$ Å, which compares favorably to the experimental values $a = 2.464$ Å and $c = 6.771$ Å [1].

3. Surfaces

As mentioned above, the most reviewed graphite surface plane is (0001) [2,3,4,5,6,7,8]. Its structure is readily extracted from the bulk as shown in Fig. 1. Without defects no reconstruction has been reported. The (0001) surface energy obtained with the present computational setup (0.18 J/m 2) is in the range of theoretical values reported in the literature (0.07 – 0.19 J/m 2) [7,44,45,46,47].

3.1. Non-reconstructed surfaces

In Fig. 2 the relaxed structures of the selected surfaces are shown. All top-layer carbon atoms are two-fold coordinated. Other surface terminations which are not expected to be stable from chemical intuition due to the presence of dangling bonds were omitted from our study. While surfaces (10 $\bar{1}$ 0) and (10 $\bar{1}$ 1) (2(a) and 2(b)) consist of nanoribbons with a zig-zag top layer, the (11 $\bar{2}$ 0) (2(c)) and (11 $\bar{2}$ 1) surfaces (2(d)) have an armchair conformation. The (10 $\bar{1}$ 0) and (11 $\bar{2}$ 0) planes are perpendicular to the **ab**-plane whereas the (10 $\bar{1}$ 1) and (11 $\bar{2}$ 1) planes are tilted.

The surface energy E_{surf} is calculated by Eq. (1). $E_{\text{slab}}^{\text{tot}}$ is the total energy of the slab, $E_{\text{bulk}}^{\text{tot}}$ is the total bulk energy, m is the number of formula units in the slab model and A_{surf} is the area of the surface unit cell.

$$E_{\text{surf}} = \frac{E_{\text{slab}}^{\text{tot}} - m \cdot E_{\text{bulk}}^{\text{tot}}}{2 \cdot A_{\text{surf}}} \quad (1)$$

The surface energies are all positive and smaller numbers denote more stable surfaces. The most important quality parameter for a slab model is the number of layers. In all cases the convergence behavior of the property of interest must be checked. In Table 1 the converged

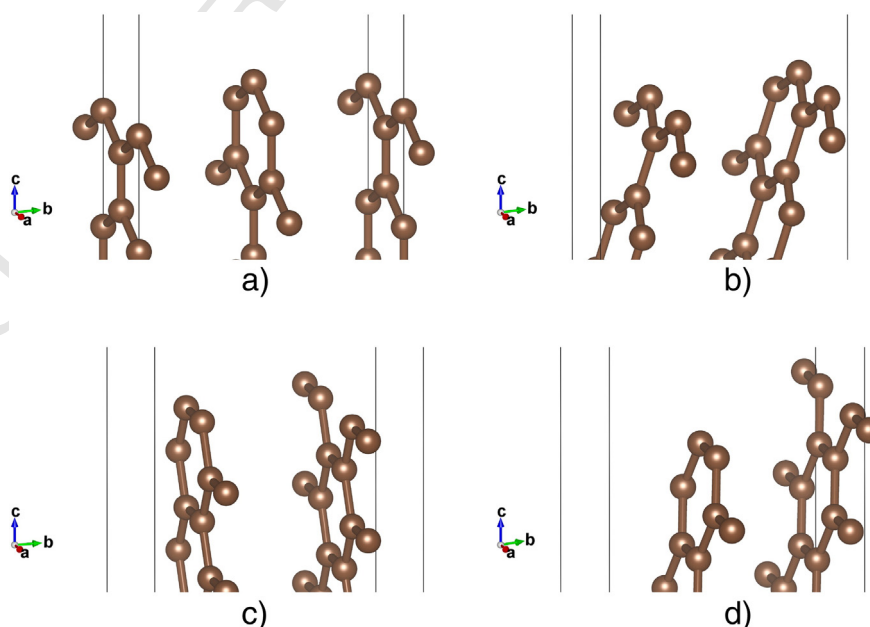


Fig. 2. Calculated structure of unreconstructed graphite surfaces (1010) 2(a), (1011) 2(b), (1120) 2(c), and (1121) 2(d).

Download English Version:

<https://daneshyari.com/en/article/5421585>

Download Persian Version:

<https://daneshyari.com/article/5421585>

[Daneshyari.com](https://daneshyari.com)